Journal of Inorganic Biochemistry 104 (2010) 1267–1275

Contents lists available at ScienceDirect

Journal of Inorganic Biochemistry

journal homepage: www.elsevier.com/locate/jinorgbio

Common basis for the mechanism of metallo and non-metallo KDO8P synthases

Peng Tao [a,b,1], H. Bernhard Schlegel [b,2], Domenico L. Gatti [a,*]

[a] Department of Biochemistry and Molecular Biology, Wayne State University School of Medicine, Detroit, Michigan 48201, United States
[b] Department of Chemistry, Wayne State University, 5101 Cass Ave Detroit, Michigan 48202, United States

ARTICLE INFO

Article history:
Received 21 February 2010
Received in revised form 10 August 2010
Accepted 11 August 2010
Available online 19 August 2010

Keywords:
KDO8PS
Metalloenzymes
Mechanism
QM/MM
Potential energy surface
Evolution

ABSTRACT

The three-dimensional structures of metal and non-metal enzymes that catalyze the same reaction are often quite different, a clear indication of convergent evolution. However, there are interesting cases in which the same scaffold supports both a metal and a non-metal catalyzed reaction. One of these is 3-deoxy-*D*-manno-octulosonate 8-phosphate (KDO8P) synthase (KDO8PS), a bacterial enzyme that catalyzes the synthesis of KDO8P and inorganic phosphate (P_i) from phosphoenolpyruvate (PEP), arabinose 5-phosphate (A5P), and water. This reaction is one of the key steps in the biosynthesis of bacterial endotoxins. The evolutionary tree of KDO8PS is evenly divided between metal and non-metal forms, both having essentially identical structures. Mutagenesis and crystallographic studies suggest that one or two residues at most determine whether or not KDO8PS requires a metal for function, a clear example of "minimalist evolution". Quantum mechanical/molecular mechanical (QM/MM) simulations of both the enzymatic and non-enzymatic synthesis of KDO8P have revealed the mechanism underlying the switch between metal and non-metal dependent catalysis. The principle emerging from these studies is that this conversion is possible in KDO8PS because the metal is not involved in an activation process, but primarily contributes to orienting properly the reactants to lower the activation energy, an action easily mimicked by amino acid side-chains.

1. Introduction

The role of metals in cellular physiology and enzyme action has been an early focus of biochemical investigation: in a 1950 review on the "Role of metal ions in enzyme systems" [1] Albert Lehninger identified three functions for metals in enzymes: 1) the metal is the actual catalytic center, 2) the metal functions as a binding group to bring enzyme and substrates in fruitful juxtaposition, 3) the metal antagonizes the effects (inhibitory or activating) of another metal in an enzyme system. Lehninger also pointed out that in some metalloenzymes the catalytic activity is inherently present already in the metallic moiety alone. For example, functions of heme proteins such as electron transfer or decomposition of hydrogen peroxide are already present in simple iron salts. However, in other cases there are no metal compounds that mimic the enzyme-catalyzed reaction. Lehninger suggested that in the first case the enzyme amplifies the intrinsic metal catalytic activity, while in the second case the metal contributes to orient the substrates in the active site, but does not have a direct catalytic role. In examples of the latter, the metal should be disposable, and one might expect the emergence in evolution of non-metallo enzymes that catalyze the same reaction.

Many enzymes that catalyze the same or similar reactions with or without metal are known. For example, fructose-biphosphate aldolase is a metallo enzyme (Class II) in *E. coli* [2], but a non-metallo enzyme (Class I) in higher eukaryotes [3–5]. Dehydrogenases are often distinguished as belonging to the Long Chain Alcohol Dehydrogenase superfamily, which typically uses zinc for catalysis, or the short chain dehydrogenase/reductase (SDR) superfamily, which uses a catalytic acid/base [6,7]. β-Lactamases can either use an active site serine to form a covalent intermediate with the antibiotic, or one or two zinc ions to activate a water molecule that attacks the β-lactam ring [8,9]. In most cases, the three-dimensional structure of the metal and non-metal enzymes that catalyze the same reaction are quite different, a clear indication of convergent evolution to a common function. However, there are interesting cases in which the same scaffold supports both a metal and a non-metal catalyzed reaction. One of these is the synthesis of 3-deoxy-*D*-manno-octulosonate 8-phosphate (KDO8P) and inorganic phosphate (P_i) from phosphoenolpyruvate (PEP), arabinose 5-phosphate (A5P), and water, catalyzed by KDO8P synthase (KDO8PS) (Fig. 1). This reaction is of significant biological relevance, as KDO8P is the phosphorylated precursor of KDO, an essential component of the endotoxin of Gram negative bacteria [10]. We and others have determined several high resolution structures for both metallo- and non-metallo forms of KDO8PS [11–15], but our structure determination of one in particular, the metal dependent *Aquifex aeolicus* (*Aa.*) enzyme, was instrumental in identifying the binding site for PEP and A5P [14]. In the absence of substrates, or when only PEP is bound, the divalent metal ion of *Aa.* KDO8PS is

* Corresponding author. Tel.: +1 313 993 4238; fax: +1 313 577 2765.
E-mail addresses: tao@chem.wayne.edu (P. Tao), hbs@chem.wayne.edu (H.B. Schlegel), dgatti@med.wayne.edu (D.L. Gatti).
[1] Tel.: +1 313 577 2546; fax: +1 313 577 8822.
[2] Tel.: +1 313 577 2562; fax: +1 313 577 8822.

0162-0134/$ – see front matter © 2010 Elsevier Inc. All rights reserved.
doi:10.1016/j.jinorgbio.2010.08.008

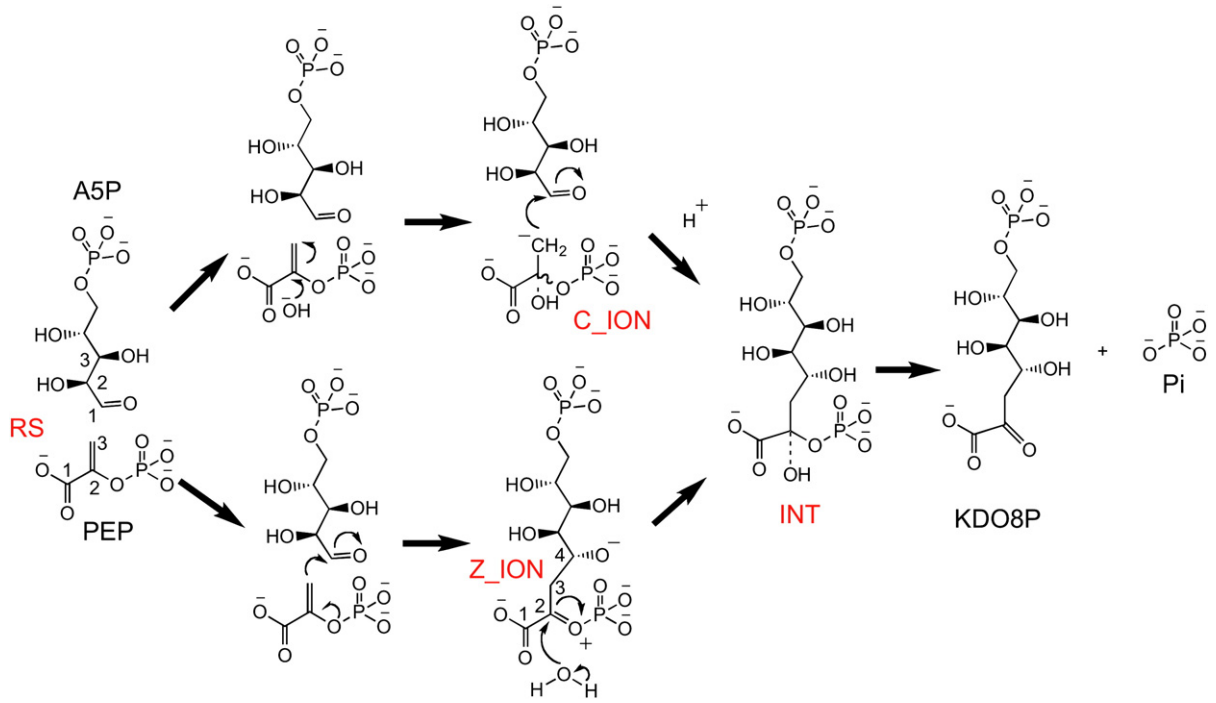

Fig. 1. KDO8P synthesis from PEP, A5P, and water. RS is the reactant state. Two stepwise mechanisms are shown requiring the formation of a transient carbanion (C_ION, upper path) or a transient zwitterion (Z_ION, lower path). Both paths converge to a linear intermediate (INT) that breaks down into KDO8P and P_i.

coordinated by the side chains of a cysteine (Cys11), a histidine (His185), a glutamic acid (Glu222), an aspartic acid (Asp233), and by a water molecule (Fig. 2A). Several metals (e.g., Cd^{2+}, Zn^{2+}, Cu^{2+}) provide comparable levels of activity [16], which is completely lost by treatment with chelators [17,18].

In the *E. coli* enzyme (a non-metallo KDO8PS) an asparagine (Asn26) replaces the metal binding cysteine and there is no metal ion; however, the other metal binding residues of the *Aa.* enzyme are conserved also in *E. coli* (His202, Glu239, and Asp250, respectively). Fersht's group [19] was the first to propose that Cys11 of *Aa.* KDO8PS is the key residue that determines whether a divalent metal is required for catalysis, and successfully converted the non-metallo *E. coli* enzyme into a metal-dependent form with the single N26C substitution, or with the double M25P/N26C substitution, which also introduced the proline present at position 10 in the *Aa.* enzyme. Similar attempts by Shulami et al. [20] with the *E. coli* enzyme gave comparable results. More recently, Cochrane et al. [15] converted the non-metallo KDO8PS from *Neisseria meningitidis* into an obligate metal-dependent form with the double substitution N23C/C246S, which reproduces the combination of Cys11 and Ser232 of *Aa.* KDO8PS. In the latter the hydroxyl moiety of Ser232 is hydrogen bonded to the sulfur of Cys11 and thus is likely to contribute to the correct orientation of this residue. Conversion of the metal-dependent *Aa.* or *Aquifex pyrophilus* KDO8PS into a metal independent form has also been accomplished with either a single C11N (Fig. 2A) or a double C11N/P10M substitution [20–22]. Thus, all the mutagenesis studies suggest that one or two residues at most determine whether KDO8PS requires a metal or not for function. As of this writing we know of 350 unique sequences of KDO8PS, of which 175 have a cysteine corresponding to Cys11 of the *Aa.* enzyme, 173 have an asparagine, and 2 have an aspartic acid. It is conceivable that after the initial choice between [cysteine + metal] and asparagine additional sequence divergence occurred to maximize activity in the structural background of the hundreds of slightly different KDO8PSs.

The fact that a switch between metal dependence and independence could be accomplished with just a single amino acid substitution represents a paradigmatic case of "minimalist engineering design". A minimalist design approach has proven to be a very successful strategy to either introduce completely new catalytic activities in an existing scaffold, or to enhance latent "promiscuous" activities [23]. It would be of great utility to know whether conversion between metal and non-metal dependent catalysis is always possible, and if possible, whether it can be achieved with minimal changes. In this report we try to unravel the principles that made such conversion possible in KDO8PS.

2. Computational methods

2.1. Potential energy surfaces

QM/MM simulations of the non-enzymatic reaction of PEP, A5P, and water were carried out with Jaguar/Qsite (Jaguar, version 7.6, Schrodinger, LLC, New York, NY, 2009). In these simulations the reactants (PEP + A5P + a single water molecule with/without Zn^{2+}/acetamide present) were initially immersed in a box (60 Å × 60 Å × 60 Å) of explicit SPC waters [24]. After an initial geometry optimization, the system was equilibrated with a short MD run for 40 ps under periodic boundary conditions and SHAKE [25] constraints. At this point all the solvent molecules farther than 26 Å from $C1^{A5P}$ were discarded. Just A5P, PEP, the single water molecule involved in the reaction, and the metal ion or the acetamide molecule were treated quantum mechanically by DFT(B3LYP) [26–29] at the lacvp* level of theory (with added "+" diffuse function only for the metal ion). In this basis set all atoms H through Ar are described with 6-31G* [30], while heavier atoms (e.g., Zn) are modeled using the LANL2DZ effective core potentials basis set [31]; the MM region, which consisted of all the other water molecules inside the sphere of 26 Å radius, was treated using the OPLS2005 force field [32]. Water molecules between 23 and 26 Å from the sphere center were restrained harmonically. Potential energy surfaces (PESs) were constructed using QM/MM calculations on a two-dimensional grid employing the forming C–O bond between the attacking water and $C2^{PEP}$, and the C–C bond between $C3^{PEP}$ and $C1^{A5P}$ as reaction coordinates. Approximately 200 points were obtained for each PES by

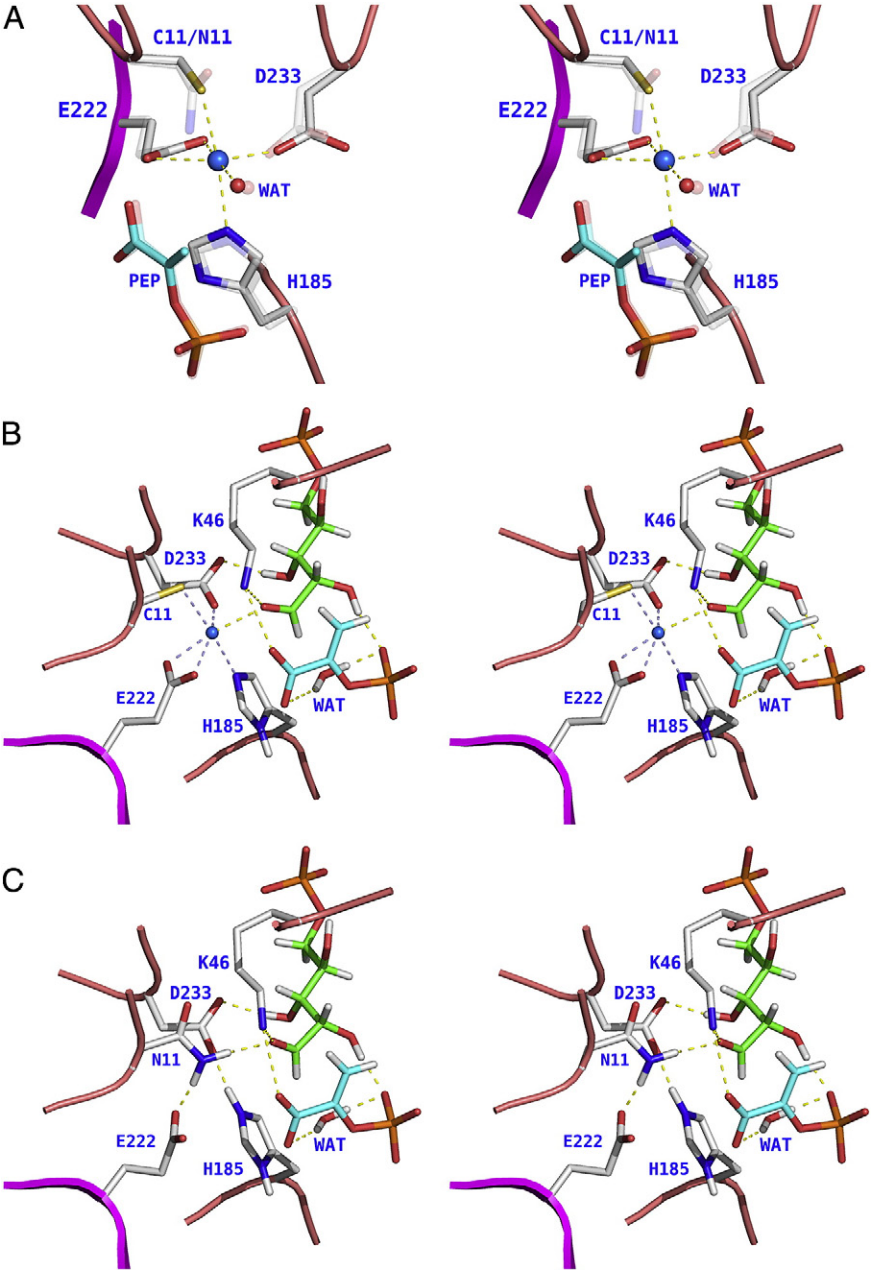

Fig. 2. Active site of metallo and non-metallo KDO8PS. A. Crystal structure of the active site of wild-type (metallo) and C11N (non-metallo) *Aa.* KDO8PS in a pre-RS state in which only PEP is bound. The wild type and the C11N mutant are shown with solid and transparent atoms/bonds, respectively. The active site metal in the wild-type enzyme is shown as a light-blue sphere. The water molecule (WAT) bound to the metal or hydrogen bonded to Asn11 is shown as a small red sphere. B,C. QM/MM optimized active sites of the wild-type (panel B) and C11N (panel C) *Aa.* KDO8PS in the reactant state (PEP + A5P + WAT). PEP is shown with cyan bonds, A5P with green bonds. The metal and its protein coordination are shown as a light-blue sphere and dashed lines. Yellow dashed lines highlight key hydrogen bonds that stabilize the relative positions of the substrates. Note the new position of the water molecule (WAT in panels B and C) displaced by the binding of A5P. There is a strong hydrogen bond between this water and the phosphate moiety of PEP, which is expected to favor the formation of the hydroxide ion that attacks $C2^{PEP}$. Also, in the absence of metal the protonated form of His185 (one of the metal ligands) is strongly stabilized with respect to its neutral counterpart (Panel C).

constraining the two grid coordinates and minimizing the energy with respect to the remaining parameters. Transition states (TSs) were refined by the quadratic synchronous transit method (QST) [33–35] utilizing two points of the surface on opposite sides of the TS. Total enthalpies (H) at 1 atm, 298.15 K for the RS, TS, and PS were calculated from the vibrational properties of the states as the sum of the total internal energy U_{tot} ($U_{tot} = QM/MM\ Energy + Zero\ Point\ Energy + U_{trans} + U_{rot} + U_{vib}$) and the pV (pressure × volume) term. A scaling factor of 0.9614 (as applicable to SCF calculations with B3LYP and 6–31G* [36]) and an inclusion threshold of 10.0 cm^{-1} were applied to vibrational frequencies prior to the calculation of thermochemical properties. Reaction and activation enthalpies (ΔH, $\Delta H^{\ddagger}$) were calculated as the differences $H^{PS} - H^{RS}$ and $H^{TS} - H^{RS}$ between the total enthalpies at the various stationary points.

2.2. NBO analysis

Atomic charges and orbital delocalizations at the stationary points of the PESs were calculated from a natural bond orbital (NBO) analysis [37] of the wave function of the quantum atoms in the QM/MM optimized geometries using the version of NBO 5.0 [38] implemented inside Jaguar/Qsite. With regard to this analysis it is important to recall that a 1-center lone pair (LP) NBO n_A is composed of a single normalized natural hybrid orbital (NHO) h_A, while a 2-center bond

(BD) NBO is a normalized linear combinations of two bonding NHOs h_A, h_B, $\Omega_{AB} = a_A h_A + a_B h_B$, with polarization coefficients a_A, a_B satisfying $a_A^2 + a_B^2 = 1$. A highly polar Ω_{AB} is identified as a lone pair n_A if 95% or more of the electron density is on a single center ($a_A^2 \geq 0.95$).

Delocalization analysis was also carried out with NBO 5.0 by examining all possible interactions between donor Lewis-type NBOs and acceptor non-Lewis NBOs, and estimating their energetic importance by 2nd-order perturbation theory. Since these interactions lead to donation of occupancy from the NBOs of the Lewis structure into unoccupied non-Lewis orbitals they represent delocalization corrections to the 0th-order natural Lewis structure. For each donor NBO (i) and acceptor NBO (j), the *2e*-stabilization energy $E(2)$ associated with delocalization is estimated as

$$E(2) = \Delta E_{ij} = q_i F(i,j)^2 / \left(\varepsilon_j - \varepsilon_i\right)$$

where q_i is the donor orbital occupancy, ε_i, ε_j are diagonal elements (orbital energies) and $F(i,j)$ is the off-diagonal NBO Fock matrix element.

2.3. Geometry optimizations

QM/MM geometry optimizations of the reactant state (RS) and of the intermediate (INT) in both metallo and non-metallo *Aa.* KDO8PS were carried out as described previously [16,39].

3. Results and discussion

3.1. PES of the reaction of PEP with A5P and water

Traditional studies of KDO8PS have established that the condensation of PEP and A5P occurs by an ordered mechanism in which PEP binds before A5P, and P_i is released before KDO8P [40–42]. The condensation step leads to the formation of a linear intermediate (INT, Fig. 1) [40,42–44]. Based on studies in which analogs of the anticipated reaction intermediate were used as inhibitors, Baasov's group [45–47] has proposed that KDO8PS forms the linear intermediate stepwise *via* a transient zwitterionic species (Z_ION in Fig. 1). On the other hand, based on several structures of wild-type and mutant *Aa.* KDO8PS [14,48,49], we have proposed that in metallo KDO8PS the metal favors the deprotonation of a water molecule to form a hydroxide ion that attacks $C2^{PEP}$; the ensuing carbanion at $C3^{PEP}$ (C_ION, Fig. 1) would then facilitate attack onto $C1^{A5P}$.

In trying to understand the role of metal in KDO8PS it is useful to consider whether Lenhinger's principle [1] applies: if the catalytic activity is already present in the metal alone, the enzyme will likely act by amplifying that intrinsic activity. Synthesis of KDO8P was reported by Baasov's group to occur in an aqueous solution at pH 5.0 with a $t_{1/2} \approx 5$ h in the presence of Zn^{2+} by intramolecular reaction of the double bond of the enolpyruvyl moiety with the aldehyde moiety in a model compound synthesized by tethering an enolpyruvyl functionality to the A5P C3–OH functionality [45].

In this reaction the metal was believed to act as a Lewis acid by activating the aldehyde carbonyl. Unfortunately, non-enzymatic synthesis of KDO8P in water from PEP and A5P, which is the exact counterpart of the reaction occurring in the enzyme, has not been studied, as this reaction is believed to be too slow or not to occur at all in the absence of KDO8PS. However, we were able to explore this reaction by quantum mechanical/molecular mechanical (QM/MM) computational methods based on density functional theory (DFT) [27,50]. The importance of comparing the enzymatic to the non-enzymatic reaction occurring inside a box of water, as opposed to using full DFT on a simpler truncated or model system in the gas-phase, has been stressed repeatedly in several studies by Warshel's group [51–53]. For this reason, the methods used in this study are similar to those used in our QM/MM simulations of both metallo and non-metallo KDO8PSs [16,39]. The PES for the non-enzymatic condensation of PEP and A5P occurring inside a sphere of water molecules of 26 Å radius was defined by two reaction coordinates: the formation of the bond between $C3^{PEP}$ and $C1^{A5P}$, and the formation of the bond between the oxygen of water and $C2^{PEP}$ (Fig. 3). PESs were calculated in the absence or presence of Zn^{2+}, and in the latter case, with Zn^{2+} coordinated in the reactant state (RS) to the water molecule that attacks $C2^{PEP}$ or to the aldehyde carbonyl oxygen of A5P. In all cases the minimum energy path on the PES leads first to a $C3^{PEP}$–$C1^{A5P}$ bond, and then to an O^{WAT}–$C2^{Z\_ION}$ bond, suggesting that in the non-enzymatic condensation of PEP and A5P, Z_ION is formed first (1st transition state, TS1), and then water reacts with it (2nd transition state, TS2): in all cases, formation of Z_ION appears to be the rate limiting step (Table 1).

Without metal the simulated reaction (Fig. 3A, PES I) is exothermic ($\Delta H = -11$ kcal/mol) with an overall barrier on the minimum energy path of ~24 kcal/mol (Table 1). The atomic charges of key atoms at the stationary points of PES I, as derived from a NBO analysis [37] of the wave function of the quantum atoms in the QM/MM optimized geometries are shown in Table 2. Second order perturbation theory analysis of the Fock matrix in NBO basis [37,54] reveals that formation of a bond between $C3^{PEP}$ and $C1^{A5P}$ at TS1 is heralded by a strong donation of orbital occupancy from a lone pair (LP) of $C3^{PEP}$ into an antibond $C1^{A5P}$–$O1^{A5P}$ orbital (Table 3). A smaller donation of orbital occupancy from the same LP into an antibond $C2^{PEP}$–OP^{PEP} orbital is also present.

In the reaction corresponding to PES II (Fig. 3B) at the RS Zn^{2+} is coordinated only by the water molecule that attacks PEP, while at TS1 and TS2 it is coordinated also by the carboxylate moiety of PEP and the carbonyl oxygen of A5P (Fig. 4). The overall reaction is endothermic ($\Delta H = +32.0$ kcal/mol) with a barrier of 35.0 kcal/mol (Table 1). NBO analysis of the wave function, in comparison with that of PES I, reveals a very different polarization of the electron density of a lone pair of $C3^{PEP}$ at TS1, with preferential donation of orbital occupancy into an antibond $C2^{PEP}$–OP^{PEP} orbital rather than into the antibond $C1^{A5P}$–$O1^{A5P}$ orbital (Table 3). There is also significant donation of orbital occupancy from a P–O bond of the phosphate moiety of PEP into an antibond O–H orbital of water and from LPs of O^{WAT} and $O1^{A5P}$ into an unoccupied LP* of the Zn^{2+} ion.

When Zn^{2+} is coordinated only to the carbonyl oxygen of A5P throughout the entire simulation (Fig. 3C, PES III), the reaction is exothermic ($\Delta H = -14$ kcal/mol) with a barrier of ~22 kcal/mol (Table 1). Overall, the shape of the PES is somewhat unusual, with an extended plateau corresponding to the progressive formation of the $C3^{PEP}$–$C1^{A5P}$ bond. Despite the lack of a clear saddle point in the PES a transition state search and the vibrational analysis identify unambiguously a single TS1, characterized by a rather large $C3^{PEP}$ to $C1^{A5P}$ distance (2.6 Å) (Fig. 4). This is the only TS in which NBO analysis of the wave function recognizes a clear double bond character in the $C2^{PEP}$–$C3^{PEP}$ bond, with significant orbital delocalization from an LP of the bridging oxygen of PEP into one of the antibond (BD*) counterparts of this double bond (Table 3). Some more modest delocalizations of orbital occupancy from lone pairs of $O1^{A5P}$ into unoccupied LP*, BD*, and RY* orbitals of Zn^{2+} and $C1^{A5P}$ are also detected.

The reaction corresponding to PES IV was studied to simulate the effect of an asparagine side chain hydrogen bonded to the carbonyl oxygen of A5P. The rationale for this investigation lies in the fact that in the active site of non-metallo KDO8PSs an asparagine side chain replaces the metal ion bound to a cysteine side chain (see above). Furthermore, a hydrogen bond between the amine moiety of Asn11 and the carbonyl oxygen of A5P or the C4–OH of INT (which originates from the carbonyl oxygen of A5P) was observed in two metal independent forms of *Aa.* KDO8PS carrying the C11N substitution [22].

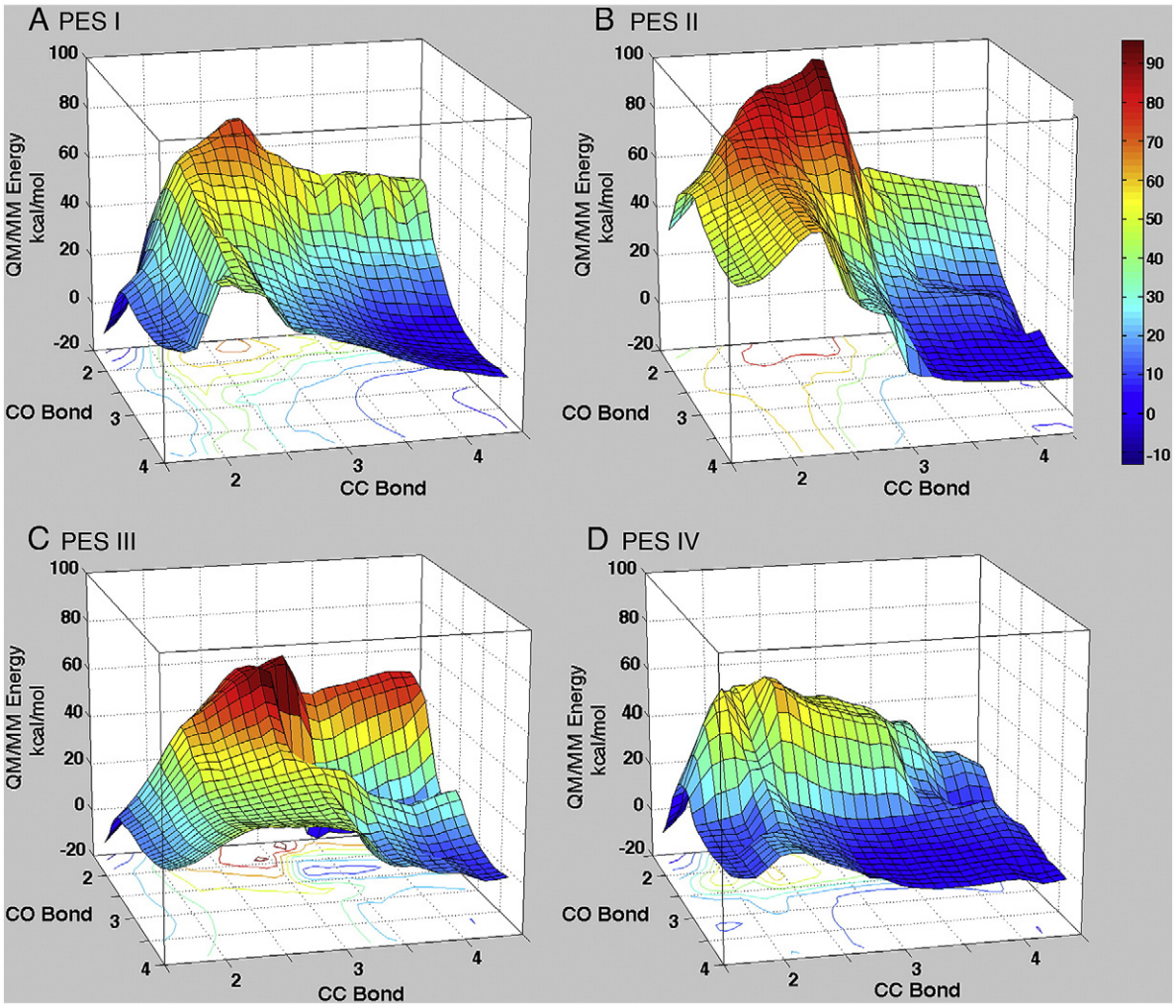

Fig. 3. PESs of the non-enzymatic condensation of PEP and A5P in water. The reactants (PEP + A5P + WAT with/without Zn^{2+}/acetamide) were immersed in a sphere of explicit waters of 26 Å radius. A5P, PEP, the single water molecule involved in the reaction, and the metal ion or the acetamide molecule were treated quantum mechanically. All the other water molecules were treated with a molecular mechanics force field. Each PES is defined by two reaction coordinates: formation of the bond between $C3^{PEP}$ and $C1^{A5P}$, and formation of the bond between the oxygen of water and $C2^{PEP}$. A. PES I: no Zn^{2+} or acetamide. B. PES II: at RS Zn^{2+} is coordinated to the water molecule that attacks $C2^{PEP}$; at TS1 and TS2 Zn^{2+} is coordinated to the same water molecule and to A5P carbonyl oxygen. C. PES III: Zn^{2+} is coordinated to A5P carbonyl oxygen. D. PES IV: acetamide (mimicking an asparagine side chain) is hydrogen bonded to A5P carbonyl oxygen. CC and CO distances are in Å, QM/MM energies are in kcal/mol. Colors on the PESs and on the projected contours below the PESs reflect QM/MM energy levels, as represented in the reference bar on the side.

We have gained some insight into the role of this asparagine side chain in the enzymatic reaction, by computing the PES of the non-enzymatic reaction in water when the amine moiety of the model compound acetamide (which mimics an asparagine side chain) is hydrogen bonded to the carbonyl oxygen of A5P (Fig. 3D, PES IV, Table 1). The simulated reaction is exothermic ($\Delta H = -11$ kcal/mol) with a first barrier of 16.9 kcal/mol corresponding to the formation of a C–C bond between $C3^{PEP}$ and $C1^{A5P}$ (TS1), and a second barrier of 5.0 kcal/mol corresponding to the formation of a C–O bond between water and Z_ION (TS2). In both TSs $C1–O^{A5P}$ or $C4–O^{Z\_ION}$ are hydrogen bonded to the amine moiety of acetamide (Fig. 4). An important feature of TS1 is the orientation of the $C2^{PEP}–C3^{PEP}$ bond with respect to the $C1^{A5P}–C2^{A5P}$ bond. These bonds are almost perpendicular to each other at TS1 in PESs I, II, and III, but perfectly co-linear at TS1 in PES IV. NBO analysis of the wave function for TS1 in PES IV reveals that this alignment causes an early formation of a covalent bond between $C3^{PEP}$ and $C1^{A5P}$ with a consequent loss of the double bond between $C1^{A5P}$ and $O1^{A5P}$. In return this lead to significant donation of orbital occupancy from $O1^{A5P}$ into antibond $C3^{PEP}–C1^{A5P}$, $O^{WAT}–H1^{WAT}$, and $N1^{ACE}–H1^{ACE}$ orbitals (Table 3).

Table 1
Calculated reaction and activation enthalpies (ΔH, $\Delta H^{\ddagger}$, in kcal/mol) in the PESs shown in Fig. 3.

	Step1: $C3^{PEP}–C1^{A5P}$ bond formation		Step 2: $O^{WAT}–C2^{Z\_ION}$ bond formation		Step 1 + Step 2	
	ΔH[a]	$\Delta H^{\ddagger}$	ΔH	$\Delta H^{\ddagger}$	ΔH	$\Delta H^{\ddagger}$
PES I	15.3	24.5	−26.3	0.8	−11.0	24.5
PES II	44.8	35.2	−12.9	11.2	31.9	35.2
PES III	5.4	21.7	−19.2	~0	−13.8	21.7
PES IV	9.4	16.9	−20.6	5.0	−11.2	16.9

[a] Total enthalpies at the stationary points of the PESs (which represent only the QM/MM energy) were calculated as described in the Computational methods section.

3.2. Role of divalent metals in the reaction of PEP with A5P and water

Altogether, the four PESs suggest that depending on which atom(s) it coordinates the metal may have either an inhibiting or a stimulating effect with respect to the reference reaction without metal. In the case in which Zn^{2+} appears to stimulate the 1st step of the reaction (PES III), the effect cannot be ascribed to its Lewis acidity and to a direct activation of the carbonyl moiety of A5P, as the expected withdrawal of electrons from the carbonyl oxygen of A5P and the consequent polarization of the

Table 2
Natural charges of key atoms at the stationary points of the PESs shown in Fig. 3.

PES I							PES II					
	RS1	TS1	TS1–RS1	RS2	TS2	TS2–RS2	RS1	TS1	TS1–RS1	RS2	TS2	TS2–RS2
$C2^{PEP}$	0.249	0.449	0.200	0.562	0.535	**−0.027**	0.192	0.398	0.206	0.581	0.536	**−0.045**
$C3^{PEP}$	−0.615	−0.625	**−0.010**	−0.574	−0.559	0.015	−0.492	−0.590	**−0.098**	−0.572	−0.556	0.016
OP^{PEP}	−0.831	−0.729	**0.102**	−0.666	−0.718	−0.052	−0.828	−0.760	**0.068**	−0.668	−0.745	−0.077
$C1^{A5P}$	0.405	0.256	**−0.149**	0.115	0.090	−0.025	0.419	0.283	**−0.136**	0.094	0.061	−0.033
$O1^{A5P}$	−0.644	−0.753	**−0.109**	−0.912	−0.910	0.002	−0.692	−0.856	**−0.164**	−1.027	−0.997	0.030
$C2^{A5P}$	−0.016	0.011	0.027	0.038	0.041	0.003	−0.017	0.023	0.040	0.056	0.053	−0.003
O^{WAT}	−1.045	−1.057	−0.012	−1.065	−1.019	**0.046**	−1.226	−1.131	0.095	−1.101	−1.002	**0.099**
PES III							PES IV					
	RS1	TS1	TS1–RS1	RS2	TS2	TS2–RS2	RS1	TS1	TS1–RS1	RS2	TS2	TS2–RS2
$C2^{PEP}$	0.213	0.314	0.101	0.572	0.540	**−0.032**	0.215	0.446	0.231	0.487	0.554	**0.067**
$C3^{PEP}$	−0.493	−0.560	**−0.067**	−0.574	−0.562	0.012	−0.500	−0.601	**−0.101**	−0.598	−0.570	0.028
OP^{PEP}	−0.851	−0.795	**0.056**	−0.644	−0.725	−0.081	−0.861	−0.731	**0.130**	−0.721	−0.729	−0.008
$C1^{A5P}$	0.435	0.379	**−0.056**	0.092	0.072	−0.020	0.426	0.236	**−0.190**	0.192	0.101	−0.091
$O1^{A5P}$	−0.661	−0.790	**−0.129**	−0.995	−0.983	0.012	−0.600	−0.803	**−0.203**	−0.851	−0.950	−0.099
$C2^{A5P}$	−0.040	−0.003	0.037	0.053	0.045	−0.008	−0.029	0.034	0.063	0.040	0.059	0.019
O^{WAT}	−1.087	−1.072	0.015	−1.077	−0.950	**0.127**	−1.078	−1.091	−0.013	−1.078	−0.962	**0.116**

Atomic charges of the RS and TS states were calculated from a Natural Bond Orbital (NBO) analysis of the wave function of the quantum atoms. RS2 is the stationary point between TS1 and TS2, in which Z_ION is about to react with water. OP is the carbon-phosphate bridging oxygen of PEP. Changes in atomic charges between reactant and transition states are shown in the columns labeled TS1–RS1 and TS2–RS2. Changes most relevant to the formation of TS1 and TS2 are in bold.

$C1^{A5P}$–O^{A5P} bond (which would favor a nucleophilic attack of $C3^{PEP}$ on $C1^{A5P}$) are very modest (Table 2). In general, the carbonyl moiety of A5P becomes more negative and the bridging oxygen of PEP more positive at the TS for the formation of the $C3^{PEP}$–$C1^{A5P}$ bond (TS1) (consistent with the predicted zwitterionic nature of Z_ION), and the oxygen of water becomes more positive at the TS for the formation of the O^{WAT}–$C2^{Z\_ION}$ bond (TS2). This pattern is common to all simulations, regardless of the presence of metal or of its coordination geometry.

Table 3
Most significant orbital delocalizations (from donor to acceptor) for key atoms at TS1 as derived from a second order perturbation theory analysis of the Fock matrix in NBO basis.

Donor NBO	Acceptor NBO	$E(2)$ stabilization energy (kcal/mol)
PES I		
LP(1) $C3^{PEP}$	BD*(2) $O1^{A5P}$–$C1^{A5P}$	197.56
LP(1) $C3^{PEP}$	BD*(2) $C2^{PEP}$–OP^{PEP}	118.46
LP(2) $O1^{A5P}$	BD*(1) O^{WAT}–$H1^{WAT}$	16.93
LP(2) $O1^{A5P}$	BD*(1) $C1^{A5P}$–$H1^{A5P}$	16.13
BD(2) O^{A5P}–$C1^{A5P}$	LP(1) $C3^{PEP}$	13.97
LP(1) $O1^{A5P}$	RY*(1) $C1^{A5P}$	11.39
PES II		
LP(1) $C3^{PEP}$	BD*(2) $C2^{PEP}$–OP^{PEP}	202.76
LP(1) $C3^{PEP}$	BD*(2) $O1^{A5P}$–$C1^{A5P}$	175.85
BD(2) P^{PEP}–$OP2^{PEP}$	BD*(1) O^{WAT}–$H2^{WAT}$	104.37
LP(2) O^{WAT}	LP*(6) Zn	42.64
LP(2) $O1^{A5P}$	LP*(6) Zn	28.81
PES III		
LP(2) OP^{PEP}	BD*(2) $C2^{PEP}$–$C3^{PEP}$	27.02
BD(2) $C2^{PEP}$–$C3^{PEP}$	BD*(2) $O1^{A5P}$–$C1^{A5P}$	17.40
LP(2) $O1^{A5P}$	BD*(1) $C1^{A5P}$–$H1^{A5P}$	14.61
LP(1) $O1^{A5P}$	RY*(1) $C1^{A5P}$	10.71
LP(1) $O1^{A5P}$	LP*(6) Zn	7.88
PES IV		
LP(3) $O1^{A5P}$	BD*(1) $C3^{PEP}$–$C1^{A5P}$	42.88
BD(1) $C3^{PEP}$–$C1^{A5P}$	BD*(2) $C2^{PEP}$–OP^{PEP}	28.24
LP(1) $O1^{A5P}$	BD*(1) $N1^{ACE}$–$H1^{ACE}$	14.55
LP(2) $O1^{A5P}$	BD*(1) O^{WAT}–$H1^{WAT}$	13.23
LP(1) $O1^{A5P}$	RY*(1) $C1^{A5P}$	10.55

LP, lone pair; BD, bond; RY, Rydberg; ACE, acetamide. The orbital number is in parenthesis; a "*" next to the orbital type indicates an unfilled valence or extra-valence orbital. OP is the carbon-phosphate bridging oxygen of PEP. OP2 is one of the oxygen atoms of the phosphate moiety of PEP.

Thus, the simulations suggest that other factors may play more important roles in the energetics of the non-enzymatic condensation of PEP and A5P in water. For example, at TS1 and TS2 of PESs I–II the dihedral angle between the C2–C3 double bond and the C–O double bond of the carboxylate moiety of PEP is significantly different from 0° (Fig. 4). In contrast, at the TSs of PESs III–IV the C2–C3 double bond and the C–O double bond of the carboxylate moiety of PEP are almost co-linear (Fig. 4). It has been theorized that the relative orientations of the two planes in which the C–C and C–O double bonds reside control the reactivity of $C3^{PEP}$ toward $C1^{A5P}$, with maximal activation when the two plane are perpendicular [55]. Our results suggest instead that maximal reactivity is achieved when the two planes are parallel. This observation is of particular importance because also in the active site of both metallo and non-metallo KDO8PSs the two planes are almost parallel [14,15,22].

Another factor is the orientation of the $C2^{PEP}$–$C3^{PEP}$ bond with respect to the $C1^{A5P}$–$C2^{A5P}$ bond. These bonds are almost perpendicular to each other at the TS1 of PESs I, II, and III, but perfectly co-linear at TS1 in PES IV. As we mentioned, NBO analysis of the wave function for TS1 in PES IV reveals that this alignment causes an early formation of a covalent bond between $C3^{PEP}$ and $C1^{A5P}$. Notably, co-linearity of the $C2^{PEP}$–$C3^{PEP}$ and $C1^{A5P}$–$C2^{A5P}$ bonds is also observed in the active site of both metallo and non-metallo KDO8PS [14,22] (see also Fig. 2).

Altogether, the simulations of the non-enzymatic condensation of PEP, A5P in water suggest that a metal ion or an asparagine side chain do not stimulate directly the reaction by activating the carbonyl oxygen of A5P during the formation of the $C3^{PEP}$–$C1^{A5P}$ bond. Furthermore, neither the metal nor asparagine appear to be involved in activating water prior to the formation of the O^{WAT}–$C2^{Z\_ION}$ bond (TS2), as the barrier at TS2 is not lowered by the presence of Zn^{2+} or acetamide in the simulations (Table 1). These simulations of the non-enzymatic reaction are consistent with our QM/MM studies of wild-type Cd^{2+} or Zn^{2+} *Aa.* KDO8PS, which suggest that also in the condensed phase of the enzyme active site the metal is not involved in water activation [16]. Instead it appears that a common role for the metal or an asparagine side chain is to orient properly the substrates in the enzyme active sites, in such a way that the more important requirements for the stimulation of catalysis (e.g., co-linearity of the carboxylate moiety of PEP with the $C2^{PEP}$–$C3^{PEP}$ double bond, and of this latter with the $C1^{A5P}$–$C2^{A5P}$ bond) are met.

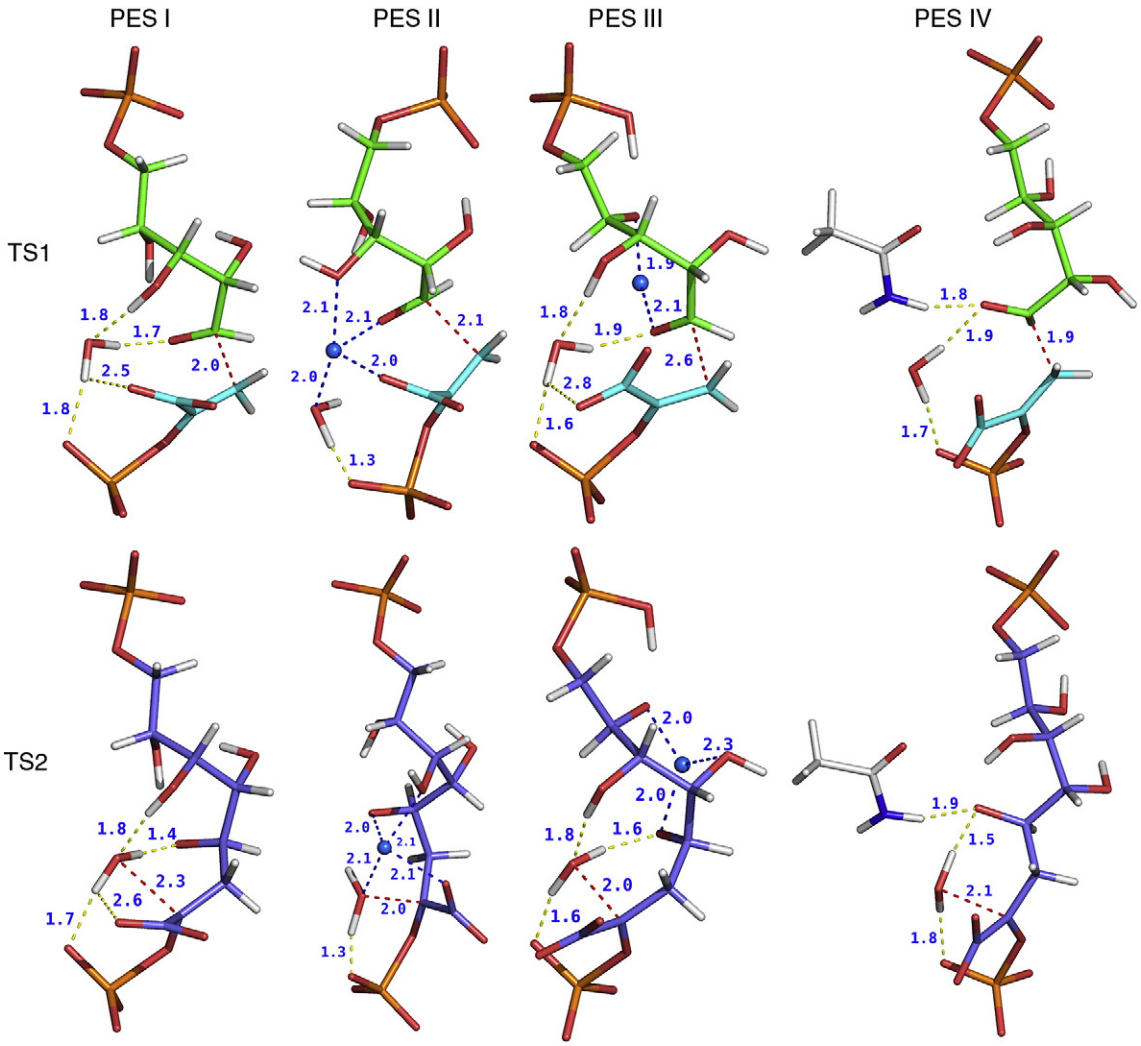

Fig. 4. Transition states in the non-enzymatic condensation of PEP and A5P in water. The relative positions of PEP, A5P, Z_ION, Zn^{2+}, water, and acetamide at TS1 (top row) and TS2 (bottom row) are shown for the PESs (I to IV, from left to right) of Fig. 3. PEP is shown with cyan bonds, A5P with green bonds, Z_ION with purple bonds, acetamide with white bonds. Zn^{2+} is shown as a light-blue sphere. Hydrogen bonds are shown as yellow dashed lines. Zn^{2+} coordination is shown as blue dashed lines. Red dashed lines represent the $C3^{PEP}$–$C1^{A5P}$ bond (TS1) or the O^{WAT}–$C2^{Z\_ION}$ bond (TS2) and reflect a pure bond-stretching mode corresponding to the single imaginary frequency identified at TS1 and TS2. Distances in Angstroms are shown next to each line.

This point of view is supported by computational studies of wild-type *Aa.* KDO8PS and of its corresponding non-metallo C11N mutant form, in which the active site geometries at the RS and INT states were refined by QM/MM methods. Fig. 2B and C shows that at the RS, PEP and A5P sit in the active site in almost identical positions in both the metal and non-metal enzyme. It should be noted that in the QM/MM optimized RS the water on the *si* side of $C2^{PEP}$ (WAT in Fig. 2B and C) is not bound to the metal or hydrogen bonded to Asn11, as in the pre-RS state (Fig. 2A), when PEP is bound in the absence of A5P. This means that upon entering the active site A5P displaces this water from its original position such that the carbonyl oxygen of A5P directly replaces the water oxygen in its coordination with the metal (Fig. 2B) or in its hydrogen bond with the amine moiety of Asn11 (Fig. 2C). The new position of the water molecule (shown in Fig. 2B and C) favors its deprotonation by the phosphate moiety of PEP to form the hydroxide ion that attacks $C2^{Z\_ION}$. In this new position the $C2^{PEP}$ to O^{WAT} distance shortens from ~3.7 to ~3.2 Å and the angles made by the $C2^{PEP}$–O^{WAT} axis with the $C1^{PEP}$–$C2^{PEP}$ and $C2^{PEP}$–$C3^{PEP}$ bonds (which reflect the anticipated attack angle) change respectively from ~88° and ~73° to ~90° and ~118°. It is worth noting that in several X-ray structures of both metallo and non-metallo forms of *Aa.* KDO8PS [14,22] there is a water molecule also on the *re* side of $C2^{PEP}$, which potentially might lead to an *anti* addition of water and A5P to PEP. While involvement of this water in the reaction has been ruled out by QM/MM simulations of the non-metallo enzyme [39], conclusive experimental or computational evidence that water attacks $C2^{PEP}$ from the *si* side also in the metallo enzyme is still lacking.

The QM/MM optimized structures of metal- and non-metal KDO8PS show remarkable similarity also in the INT state (Fig. 5A and B), in which the active site metal or the amine moiety of Asn11 form a coordination or a hydrogen bond with $C4–OH^{INT}$. A comparison between the RS and INT states for both forms of the enzyme also shows another important characteristic of this reaction: in both cases the enzyme moves very little between the two states (Fig. 5). This is quite in contrast with the large changes that occur in the solvent surrounding the reactants when the non-enzymatic reaction is simulated inside a sphere of water molecules (not shown). In fact, when the structures of the QM/MM optimized RS and INT states were used to determine the reorganization energy of the active site it was found to be ~40 kcal/mol for both metallo and non-metallo engineered form of *Aa* KDO8PS, as opposed to ~160 kcal/mol for the reorganization of the solvent molecules that surround the reactants in the absence of the enzyme [39]. This calculation is consistent with the accumulated work of Warshel's group of almost two decades,

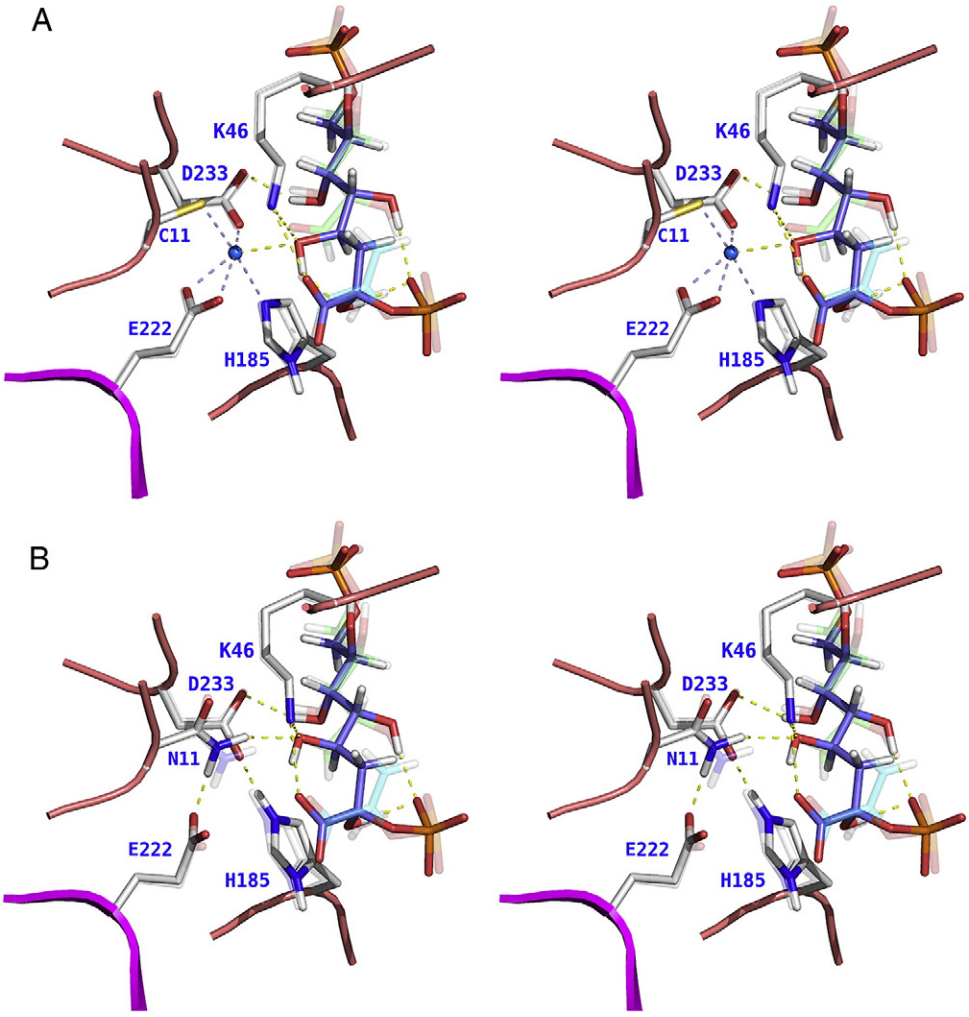

Fig. 5. QM/MM optimized active sites of wild-type and C11N *Aa.* KDO8PS with the reaction intermediate INT bound. A, wild-type; B. C11N *Aa.* KDO8PS. INT is shown with slate bonds. The corresponding reactant states, as already shown in Fig. 2B and C, are superimposed and represented with transparent atoms/bonds. Note the almost complete absence of motion in the protein between the RS and INT states.

suggesting that enzymes lower the activation energy by reorganizing their active site along the reaction coordinates much less than the corresponding reorganization of the solvent molecules when the same reaction occurs without enzyme [51,53,56].

In two separate studies [16,22], we have provided experimental evidence confirming the QM/MM simulations. For example, the structure of the Cu^{2+} substituted form of *Aa.* KDO8PS shows the C4–OH of the product KDO8P (which originates from the carbonyl oxygen of A5P) coordinated to the active site metal [16]. The structures of two metal independent forms of *Aa.* KDO8PS carrying the C11N substitution show either the carbonyl oxygen of A5P or the C4–OH of INT hydrogen bonded to the amine moiety of the side chain of Asn11 [22]. As shown in Fig. 2A, this amine moiety occupies the same position in the active site of metal-independent KDO8PSs as the metal ion in metal-dependent KDO8PSs. Thus, in different experimental structures of the metal and of the engineered non-metal forms of *Aa.* KDO8PS, at three different stages of catalysis (RS, INT, and KDO8P) the carbonyl oxygen of the A5P functionality appears to be either coordinated to the active site metal, or hydrogen bonded to Asn11 (which is the same result obtained by the QM/MM simulations). These observations help rationalize why removal of the active site metal from metallo KDO8PS [17,20,57], or replacement of Asn11 with other types of residues in non-metallo KDO8PS [57] are so deleterious for function: most likely these changes disturb the correct alignment of A5P and water with respect to PEP, which is so critical for lowering the activation energy of the reaction. It should be noticed however, that the catalytically active conformation of A5P described here must be a transient one: in fact, direct binding of the A5P carbonyl to the active site metal has not been observed yet in metallo KDO8PSs, and in the engineered metal-independent forms of KDO8PS, in addition to the favorable conformation, A5P is often observed (for example, in different active sites of the same tetrameric enzyme) in conformations that are not likely to directly precede the reaction, as the *si* face instead of the *re* face of the aldehyde is presented to PEP [22], contrary to the established stereochemistry of the reaction [42,43].

4. Conclusions

As of this writing, we have computed a complete PES of the reaction in the active site of KDO8PS only for the non-metallo enzyme [39], and it turned out to be similar to that computed for the same reaction inside a sphere of water molecules, without enzyme and with added acetamide (Figs. 3D and 4). The non-enzymatic reaction is predicted to be clearly step-wise (Figs. 3–4, Table 1) with formation of a transient oxocarbenium ion (Z_ION, lower path in Fig. 1), while the enzymatic reaction is predicted to have at least a partial character of a concerted reaction between PEP, A5P, and water [39]. In both cases, formation of the $C3^{PEP}$–$C1^{A5P}$ bond represents the bottleneck of the reaction. Altogether, these results confirm the original proposals and experimental work of Baasov's group [20,45,47].

QM/MM studies of this reaction either in solution, with key chemical groups mimicking the catalytic side chains, or with a complete simulation of the non-metallo enzyme active site suggest that a role equivalent to that of the metal is performed by an asparagine side chain that in the non-metallo form of the enzyme replaces the combination cysteine + metal. While a complete simulation of the reaction in the metallo enzyme is not available yet, the QM/MM optimized geometries of the RS and INT states for both enzyme forms suggest that the active site metal or the amine moiety of Asn11 stimulate the reaction by positioning A5P and water in a similar way (Fig. 2B,C) with respect to PEP in both metallo and non-metallo KDO8PSs.

The evolution of almost identical metal dependent and metal-independent forms of KDO8PS was possible because the metal does not appear to be directly involved in an activation process, but primarily contributes to stabilize the relative positions and conformations of the reactants that allow for the lowest activation energy. Thus, if a general conclusion can be drawn from these studies, it would be that, following Lehninger's original suggestion, attempts to convert metallo-enzymes to non-metallo forms or *vice versa* should focus on clarifying whether the metal has a direct activating role or just contributes to orient the substrates in the active site. The accumulated results from mutagenesis, crystallographic and computational studies of KDO8PS suggest that a minimalist strategy to achieve this conversion is more likely to succeed in the latter case.

Abbreviations

KDO8P	3-deoxy-*D*-*manno*-octulosonate 8-phosphate
KDO8PS	3-deoxy-*D*-*manno*-octulosonate 8-phosphate synthase
PEP	phosphoenolpyruvate
A5P	arabinose 5-phosphate
ACE	acetamide
C_ION	carbanion intermediate
Z_ION	zwitterion intermediate
INT	tetrahedral intermediate
RS	reactant state
PS	product state
TS	transition state
DFT	density functional theory
QM	quantum mechanics
MM	molecular mechanics
MD	molecular dynamics
PES	potential energy surface
NBO	natural bond orbital
LP	lone pair
BD	bond
RY	Rydberg
ps	picoseconds

Acknowledgments

This work was supported by PHS Grant GM69840 to D.L.G., by NSF Grant CHE0512144 to H.B.S., and by a Wayne State University Research Enhancement Program in Computational Biology Grant to D.L.G. and H.B.S.

References

[1] A.L. Lehninger, Physiol. Rev. 30 (1950) 393–429.
[2] S.J. Cooper, G.A. Leonard, S.M. McSweeney, A.W. Thompson, J.H. Naismith, S. Qamar, A. Plater, A. Berry, W.N. Hunter, Structure 4 (1996) 1303–1315.
[3] H. Kim, U. Certa, H. Dobeli, P. Jakob, W.G.J. Hol, Biochemistry 37 (1998) 4388–4396.
[4] S.J. Gamblin, B. Cooper, J.R. Millar, G.J. Davies, J.A. Littlechild, H.C. Watson, FEBS Lett. 262 (1990) 282–286.
[5] G. Hester, O. Brenner-Holzach, F.A. Rossi, M. Struck-Donatz, K.H. Winterhalter, J.D.G. Smit, K. Piontek, FEBS Lett. 292 (1991) 237–242.
[6] Z. Krozowski, J. Steroid Biochem. Mol. Biol. 51 (1994) 125–130.
[7] J.M. Jez, M.J. Bennett, B.P. Schlegel, M. Lewis, T.M. Penning, Biochem. J. 326 (1997) 625–636.
[8] J.F. Fisher, S. Mobashery, Curr. Protein Pept. Sci. 10 (2009) 401–407.
[9] C. Bebrone, Biochem. Pharmacol. 74 (2007) 1686–1701.
[10] C.R. Raetz, C. Whitfield, Annu. Rev. Biochem. 71 (2002) 635–700.
[11] H.S. Duewel, R.W. Woodard, J. Biol. Chem. 275 (2000) 22824–22831.
[12] T. Wagner, R.H. Kretsinger, R. Bauerle, W.D. Tolbert, J. Mol. Biol. 301 (2000) 233–238.
[13] S. Radaev, P. Dastidar, M. Patel, R.W. Woodard, D.L. Gatti, J. Biol. Chem. 275 (2000) 9476–9484.
[14] H.S. Duewel, S. Radaev, J. Wang, R.W. Woodard, D.L. Gatti, J. Biol. Chem. 276 (2001) 8393–8402.
[15] F.C. Cochrane, T.V. Cookson, G.B. Jameson, E.J. Parker, J. Mol. Biol. 390 (2009) 646–661.
[16] F. Kona, P. Tao, P. Martin, X. Xu, D.L. Gatti, Biochemistry 48 (2009) 3610–3630.
[17] H.S. Duewel, G.Y. Sheflyan, R.W. Woodard, Biochem. Biophys. Res. Commun. 263 (1999) 346–351.
[18] C. Furdui, L. Zhou, R.W. Woodard, K.S. Anderson, J. Biol. Chem. 279 (2004) 45618–45625.
[19] Z. Oliynyk, L. Briseno-Roa, T. Janowitz, P. Sondergeld, A.R. Fersht, Protein Eng. Des. Sel. 17 (2004) 383–390.
[20] S. Shulami, C. Furdui, N. Adir, Y. Shoham, K.S. Anderson, T. Baasov, J. Biol. Chem. 279 (2004) 45110–45120.
[21] J. Li, J. Wu, A.S. Fleischhacker, R.W. Woodard, J. Am. Chem. Soc. 126 (2004) 7448–7449.
[22] F. Kona, X. Xu, P. Martin, P. Kuzmic, D.L. Gatti, Biochemistry 46 (2007) 4532–4544.
[23] M.D. Toscano, K.J. Woycechowsky, D. Hilvert, Angew. Chem. Int. Ed Engl. 46 (2007) 3212–3236.
[24] H.J.C. Berendsen, J.P.M. Postma, W.F. van Gunsteren, J. Hermans, in: B. Pullman (Ed.), Intermolecular Forces, Reidel, Dordrecht, 1981, pp. 331–342.
[25] J.-P. Ryckaert, G. Ciccotti, H.J.C. Berendsen, J. Comput. Phys. 23 (1977) 327–341.
[26] P. Geerlings, F. De Proft, W. Langenaeker, Chem. Rev. 103 (2003) 1793–1874.
[27] R.G. Parr, W. Yang, Density-Functional Theory of Atoms and Molecules, Oxford University Press, Oxford, 1989.
[28] A.D. Becke, J. Chem. Phys. 98 (1993) 5648–5652.
[29] P.J. Stephens, F.J. Devlin, C.F. Chabalowski, M.J. Frisch, J. Phys. Chem. 98 (1994) 11623–11627.
[30] V.A. Rassolov, M.A. Ratner, J.A. Pople, P.C. Redfern, L.A. Curtiss, J. Comput. Chem. 22 (2001) 976–984.
[31] P.J. Hay, W.R. Wadt, J. Chem. Phys. 82 (1985) 299–310.
[32] W.L. Jorgensen, J. Tirado-Rives, J. Am. Chem. Soc. 110 (1988) 1657–1666.
[33] T.A. Halgren, W.N. Lipscomb, Chem. Phys. Lett. 49 (1977) 225–232.
[34] A. Jensen, Theor. Chim. Acta 63 (1983) 269–290.
[35] S. Bell, J.S. Crighton, J. Chem. Phys. 80 (1984) 2464–2475.
[36] A.P. Scott, L. Radom, J. Phys. Chem. 100 (1996) 16502–16513.
[37] F. Weinhold, in: N.L. Allinger, P.v.R. Schleyer, T. Clark, J. Gasteiger, P.A. Kollman, H.F. Schaefer III, P.R. Schreiner (Eds.), Encyclopedia of Computational Chemistry, Vol. 3, John Wiley & Sons, Chichester, UK, 1988, pp. 1792–1811.
[38] E.D. Glendening, J.K. Badenhoop, A.E. Reed, J.E. Carpenter, J.A. Bohmann, C.M. Morales, F. Weinhold, Theoretical Chemistry Institute - University of Wisconsin, Madison, , 2001.
[39] P. Tao, D.L. Gatti, H.B. Schlegel, Biochemistry 48 (2009) 11706–11714.
[40] L. Hedstrom, R. Abeles, Biochem. Biophys. Res. Commun. 157 (1988) 816–820.
[41] A. Kohen, A. Jakob, T. Baasov, Eur. J. Biochem. 208 (1992) 443–449.
[42] A. Kohen, R. Berkovich, V. Belakhov, T. Baasov, Bioorg. Med. Chem. Lett. 3 (1993) 1577–1582.
[43] G.D. Dotson, P. Nanjappan, M.D. Reily, R.W. Woodard, Biochemistry 32 (1993) 12392–12397.
[44] G.D. Dotson, R.K. Dua, J.C. Clemens, E.W. Wooten, R.W. Woodard, J. Biol. Chem. 270 (1995) 13698–13705.
[45] S. Du, D. Plat, V. Belakhov, T. Baasov, J. Org. Chem. 62 (1997) 794–804.
[46] L. Kaustov, S. Kababya, S. Du, T. Baasov, S. Gropper, Y. Shoham, A. Schmidt, Biochemistry 39 (2000) 14865–14876.
[47] O. Asojo, J. Friedman, N. Adir, V. Belakhov, Y. Shoham, T. Baasov, Biochemistry 40 (2001) 6326–6334.
[48] J. Wang, H.S. Duewel, J.A. Stuckey, R.W. Woodard, D.L. Gatti, J. Mol. Biol. 324 (2002) 205–214.
[49] X. Xu, F. Kona, J. Wang, J. Lu, T. Stemmler, D.L. Gatti, Biochemistry 44 (2005) 12434–12444.
[50] H. Lin, D.G. Truhlar, Theor. Chem. Acc. 117 (2007) 185–199.
[51] A. Warshel, W.W. Parson, Q. Rev. Biophys. 34 (2001) 563–679.
[52] A. Warshel, P.K. Sharma, M. Kato, W.W. Parson, Biochim. Biophys. Acta 1764 (2006) 1647–1676.
[53] A. Warshel, P.K. Sharma, M. Kato, Y. Xiang, H. Liu, M.H. Olsson, Chem. Rev. 106 (2006) 3210–3235.
[54] F. Weinhold, C.R. Landis, Bonding Valency, A natural bond orbital donor-acceptor perspective, Cambridge University Press, Cambridge, 2005.
[55] Y. Li, J.N. Evans, Proc. Natl Acad. Sci. USA 93 (1996) 4612–4616.
[56] A.J. Smith, R. Muller, M.D. Toscano, P. Kast, H.W. Hellinga, D. Hilvert, K.N. Houk, J. Am. Chem. Soc. 130 (2008) 15361–15373.
[57] S. Shulami, O. Yaniv, E. Rabkin, Y. Shoham, T. Baasov, Extremophiles 7 (2003) 471–481.